Acta Physiol Plant (2016) 38:240
DOI 10.1007/s11738-016-2256-x

ORIGINAL ARTICLE

ASYMMETRIC LEAVES2-LIKE15 gene, a member of *AS2/LOB* family, shows a dual abaxializing or adaxializing function in *Arabidopsis* lateral organs

Lai-Sheng Meng[1] · Zhi-Bo Wang[2] · Xiao-Ying Cao[1] · Hua-Juan Zhang[1] · Yi-Bo Wang[2] · Ji-Hong Jiang[1]

Received: 18 March 2016 / Revised: 18 August 2016 / Accepted: 4 September 2016 / Published online: 10 September 2016

Abstract In determining leaf adaxial fates, *Arabidopsis ASYMMERTIC LEAVES1* (*AS1*) and *AS2/LBD6* are essential. The *Arabidopsis ASYMMETRIC LEAVES2-LIKE15/LBD17* gene, one member of the *LATERAL ORGAN BOUNDARY DOMAIN* gene family, is expressed at the base of juvenile lateral roots, as well as in boundaries between meristems and organ primordial. For better comprehending the function of *ASL15/LBD17* in the *Arabidopsis* development, its antisense-expression construct was constructed, and some *35S:ASL15/LBD17* transgenic plants that were antisense overexpression mutants were attained. The transgenic plants can specify either abaxial or adaxial cell fate in differently shaped rosette leaves. In detail, slightly and extremely narrow rosette leaves (class I) displayed abaxial cell traits, compared with those of Col-0. Inflorescence stems of these transgenic plants also showed abaxial organ identity. Both radial needle-like and filamentous symmetric rosette leaves (class II) presented adaxial cell fate, in contrast to those of wild type (Col-0). However, in the background of *AS2* mutation, antisense *35S:ASL15* only presented abaxial organ identity, implying that the influences of antisense *35:ASL15* require a functional *AS2* gene. In addition, antisense *35S:ASL15* was defective in proximodistal patterning. In addition, antisense *35S:ASL15* lead to the enhancement of the transcript levels of the *KNOX* genes, i.e., *KNAT2*, *KNAT6,* and *STM,* but not of the related *KNAT1* gene. Taken together, our findings show that *ASL15/LBD17* has a dual abaxializing or adaxializing function, and is also related to distal and proximal patterning in the lateral organs of *Arabidopsis*. Therefore, *ASL15/LBD17* has multiple functions in the *Arabidopsis* development.

Keywords *ASL15/LBD17* · Antisense · Adaxial/abaxial polarity · *Arabidopsis* · *LBD* gene family

Introduction

In shoot apical meristem (SAM), the peripheral zone is formed from the leaf primordium. The proximodistal, mediolateral, and abaxial/adaxial axes are established with leaf primordia formation (Hudson 2000).

Recently, many studies have proved a few genes that play important roles in establishing leaf ab/adaxial patterning. In the class III homeodomain/Leu zipper (*HD-ZIP*) family, five members can control leaf adaxial patterning (Prigge et al. 2005; Zhong and Ye 2004; Emery et al. 2003; McConnell et al. 2001; McConnell and Barton 1998). With these gene mRNAs targeted via two micro-RNAs (miR166 and miR165), their downregulation can be defined in abaxial cells (Williams et al. 2005; Kim et al. 2005; Bao et al. 2004; Tang et al. 2003). The *as2* alleles in the Landsberg *erecta* (L*er*) background induce the transformation of adaxial cell type into partially abaxial cell type (Xu et al. 2003), whereas transgenic plants with *35S:AS2*

Communicated by J Gao.

✉ Lai-Sheng Meng
menglsh@jsnu.edu.cn

✉ Ji-Hong Jiang
jhjiang@jsnu.edu.cn

[1] The Key Laboratory of Biotechnology for Medicinal Plant of Jiangsu Province, School of Life Science, Jiangsu Normal University, Xuzhou 221116, Jiangsu, People's Republic of China

[2] School of Bioengineering and Biotechnology, Tianshui Normal University, Tianshui 741001, People's Republic of China

present almost either adaxialized or radial leaves (Xu et al. 2003; Lin et al. 2003). The, *bop1* and *bop2,* double mutants partially exhibit the transformation of adaxial cell type into abaxial cell type (Ha et al. 2007). On the other hand, both the members of *KANADI* (*KAN*) gene family and the members of *YABBY* (*YAB*) gene family can function in abaxial patterning (Eshed et al. 2004; Emery et al. 2003; Sawa et al. 1999; Eshed et al. 1999; Siegfried et al. 1999).

Class I *KNOX* genes function in the control of leaf patterning. There are *KNAT1*, *KNAT2*, *SHOOTMERISTEMLESS* (*STM*), and *KNAT6* in Class I *KNOX* genes of *Arabidopsis* (Chuck et al. 1996; Lincoln et al. 1994; Long et al. 1996). These genes can be significantly expressed in the *SAM*, but not in the earlier young primordia (Sentoku et al. 1999; Tamaoki et al. 1997; Nishimura et al. 1999; Long et al. 1996; Jackson et al. 1994). On the basis of the determination of leaf cell fate, it is very important that class I *KNOX* gene expression can be inhibited in both mature leaf organs and primordia. Once genes of class I *KNOX* are expressed abnormally, developmental perturbation, for example, the change of both leaf development and ectopic meristem formation, may be caused (Sentoku et al. 2000; Tamaoki et al. 1997; Chuck et al. 1996; Hareven et al. 1996; Schneeberger et al. 1995; Sinha et al. 1993; Lincoln et al. 1994).

In *Arabidopsis thaliana*, the genes of the *LBD* family are always expressed in boundaries at the bases of young lateral roots, as well as between organ primordia and meristems (Shuai et al. 2002). The abnormal expression of these genes often causes the expression change of *KNOX* genes. Loss-of-function of *AS1* and *AS2* causes the ectopic expression of *KNOX* genes in leaf blades, leading to the production of severely lobed leaves, whereas *AS2* ectopic expression suppresses the expressions of *KNOX* genes (Chalfun-Junior et al. 2005; Semiarti et al. 2001; Lin et al. 2003). Over-expressing *ASL1/LBD36* triggers the suppression of the homeobox gene *BP* (Chalfun-Junior et al. 2005). These reports indicate that the synchronous and antagonistic relationship between ASL/LBD and homeobox members might be essential to the differentiation of lateral organs.

Currently, ASL/LBD family has been well studied. The lateral organ boundaries domain (LBD) transcription factors were recently reported to be important in regulating callus formation (Fan et al. 2012). The genes of *LBD18*, *LBD17*, *LBD16*, and *LBD29* can be expressionally induced in explants cultured on MS supplemented with callus-inducing medium (CIM), and their four ectopic expression in Arabidopsis was adequate to lead to the callus formation with no supplied plant hormones. Moreover, inhibiting function of the LBD leads to the defects in callus formation (Fan et al. 2012). More interestingly, LBD16 and LBD29 are involved in cell-fate transition cooperating with *WUSCHEL-RELATED HOMEOBOX11* (*WOX11*) and *WOX12* (Liu et al. 2014).

Antisense mRNA is a very useful tool to suppress the expression of specific genes in biology (McHale and Koning 2004; Andersson et al. 2001; Oeller et al. 1991; Hamilton et al. 1990; Smith et al. 1988; Van der Krol et al. 1988; Rothstein et al. 1987; Ecker and Davis 1986); more interestingly, it is specific in the sense that only the mRNA level of the desired protein being changed, and other members of the gene family cannot be affected (Ganeteg et al. 2001; Andersson et al. 2001; Zhang et al. 1997). Here, we reported that *ASL15/LBD17* gene, one member of the *Arabidopsis LBD* gene family, can be expressed in the boundaries between organ primordia and meristems. We transformed antisense *ASL15/LBD17* gene into *Arabidopsis*, and then gained many transgenic plants with antisense *35S:ASL15/LBD17*. These findings indicate that *35S:ASL15/LBD17* specifies either abaxial or adaxial cell fate in differently shaped rosette leaf blades of *Arabidopsis*, and also displays to be defective in proximodistal patterning in the lateral organs of *Arabidopsis*.

Methods

Plant materials

In this study, we used *Arabidopsis thaliana* ecotype Columbia as research materials. Seeds were sown on MS medium with 1 % sucrose and cold-treated at 4–6 °C for 3 days. *Arabidopsis* plants were sowed and grown under 16-h-light/8-h-dark cycles with cool white fluorescent light of 100–150 pmol m^{-2} s^{-1} at 21 ± 2 °C (Meng et al. 2015a, b).

Vector construction, plant transformation

The *ASL15/LBD17* (At2g42440) coding region (a DNA fragment corresponding to nucleotides 138–701 of the full-length Arabidopsis *ASL15/LBD17*) was amplified, which derived from 12-day-old seedling cDNA of Col-0. The cDNA was inserted in the antisense orientation and placed downstream of the cauliflower mosaic virus *35S* promoter in *pBI121* vector (Fig. lb). And then, the *35S:ASL15/LBD17* construct was sequenced for confirmation.

Transgenic plants with antisense *ASL15/LBD17* construct were generated via the vacuum infiltration of Col-0 and *as2-1* Col recipient seedlings via using *Agrobacterium tumefaciens* strain *GV3101* (Meng et al. 2015a, b). These transgenic seedlings with antisense *ASL15/LBD17* construct were proved via PCR using an *nptII* reverse primers (5-aatctcgtgatggcaggttg-3) and forward primer (5-gaggctattcggctatgact-3) (Tzfira et al. 1997).

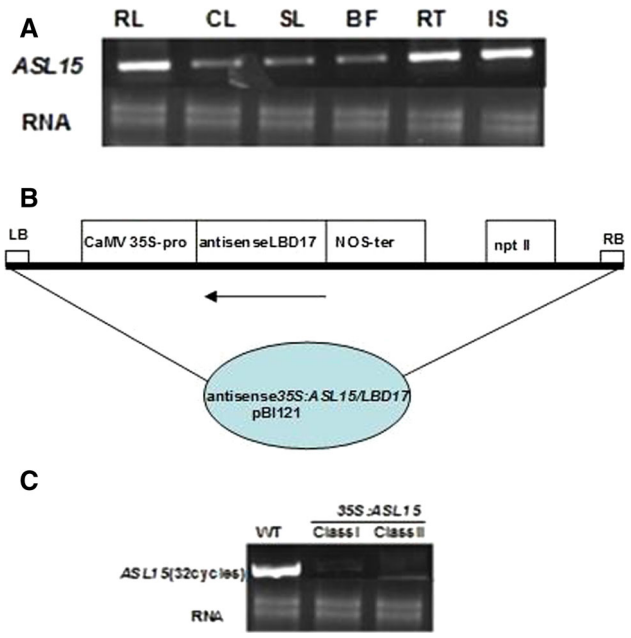

Fig. 1 Expressions of *ASL15* in wild type and *35S:ASL15/17*. **a** Representative expression level of *ASL15/LBD17* in different organ of *Arabidopsis*. *CL* cauline leaves, *RL* rosette leaves, *RT* roots, *IS* inflorescence stems, *BF* blossom flowers, *SL* siliques. **b** The used vector for the transformation of the 568-bp *Arabidopsis 35:ASL15/LBD17*cDNA antisense orientation into *Arabidopsis*. The antisense *ASL15/LBD17* cDNA insert is flanked via the transcriptional terminator at the 3′ end and via 35S (the cauliflower mosaic virus) promoter at the 5′ end. *RB* right border, *LB* left border, *nptII* neomycin phosphotransferase gene, and its expression can cause plant resistance to kanamycin. **c** Representative *ASL15/LBD17* expression is suppressed completely in class I and class II transgenic plants, in contrast to that of wild type. RNA was used as a control

Molecular analyses

Total RNA was gained via using Trizol [Sangon Biotech (Shanghai) Co., Ltd.]. To reverse transcriptase PCR research, cDNA was amplified using 1 μg of total RNA using MMuLV Reverse Transcriptase and an oligo dT 18 primers [Sangon Biotech (Shanghai) Co., Ltd.]. For PCR amplification of each cDNA, relative volume was used as a template.

The PCR primers in the CDS were as follows: *ASL15/LBD17-ASL15/LBD17-R* (5′-aaagtgttcgtcaagtgctg-3′) and *F* (5′-tgctaccaccaaatggaaat-3′). For examining the expression alternation of ab/adaxial polarity genes in transgenic plants with antisense *35S:ASL15/LBD17*, reactions of RT-PCR were performed. Gene-specific primers used were: *FIL* 5′-ttcttggcagcagcactaaa-3′ and *FIL* 5′-gctatgtccaatgcaacttt-3′, *PHB-5* 5-tgatggtccattcgatgagc-3 and *PHB-3* 5-tctaaactcacgaggccgca-3, and *YAB* 5′-tcagccatgagtccaaagtg-3′ and *YAB5*′-acttctcatctacggaccag-3′ (Lin et al. 2003). For examining the expression and the alternation of the transcript levels of the *KNOX* genes in transgenic plants with antisense *35S:ASL15/LBD17*, RT-PCR reactions were performed. Gene-specific primers used were: *KNAT1-* and *KNAT1-R* (5′-tgttgaggatgtgaatggga-3′) and *F* (5′-gctccacctgatgtggttga-3′), *STM-R* (5-tacaaactgctagtcctccg-3) and *STM-F* (5-ttagggagcctcaagcaaga-3), and *KNAT6-R* (5′-ccggtgaaaattgtgtctct-3′) and *KNAT6-F* (5′-tggcagactcgacaccagta-3′) (Lin et al. 2003); *KNAT2-R* (5′-tccgctgctatgtcatcatc-3′), *KNAT2-F* (5′-accaccggagacaatcaaag-3′) (Byrne et al. 2000).

All above PCRs were completed with denaturation at 94 °C for 5 min, followed by 32 cycles of 94 °C for 20 s, 60 °C for 20 s, 72 °C for 40 s, and a final incubation at 72 °C for 7–10 min. The above PCR products were assayed via electrophoresis on a 1.5 % agarose gel (Meng 2015; Meng and Yao 2015).

Morphological analyses

All histological experiments were performed (Meng et al. 2009). Following sample preparation, scanning electron microscopy was performed on Quanta 200 FEG SEM, which has been described by Alvarez et al. (1992). *FIL* probe was generated via synthesizing DIG-labeled antisense RNA and linearizing cDNA plasmids using T7 RNA polymerase. *FIL* probes were generated, which has been described by Eshed et al. (2001).

Results

Identification of *Arabidopsis* transgenic plants with antisense *35S:ASL15/LBD17* construct

The *ASL15/LBD17* gene transcripts can be detected in all tissues of wild-type Columbia plants, such as rosette leaves, cauline leaves, roots, inflorescence stems, siliques, and blossom flowers (Fig. 1a). *ASL15/LBD17* transcripts were detected to express abundant in rosette leaves than cauline leaves. For elucidating the role of *ASL15/LBD17* gene in the growth and development of *Arabidopsis*, we constructed the antisense expression of the *LBD17* gene under the control of 35S promoter from *Cauliflower mosaic virus* (Fig. 1b). Transgenic plants were generated via the transformation of the antisense *35S:LBD17* transgene constructs to the Col-0 using vacuum infiltration (Meng et al. 2015a, b). Relative transgenic seedlings were proved via PCR of the *nptII* reporter gene using specific reverse primer (5′-aatctcgtgatggcaggttg-3′) and forward primer (5′-gaggctattcggctatgact-3′) (Tzfira et al. 1997). We can prove that the specific DNA product of *npt II* gene (804 bp), as assayed via PCR, was only revealed in transgenic seedlings, but not in Col-0 (data not shown). In 82 identified transgenic

seedlings, they showed significantly phenotype defects that can be categorized into two classes. Thirty-eight independent class I seedlings were slightly altered. They exhibited slightly (20/38) and extremely (18/38) narrow rosette leaf blades, and round cauline leaf blades with short petiole (Figs. 2a, c, e, f arrow; 3m arrow). Twenty-six independent class II seedlings were the most severely influenced. They presented radially needle-like (17/26) and either filamentous symmetric or needle-like rosette leaf blades (9/26) (Fig. 2d arrow). While 18 identified transgenic seedlings do not grow aberrant rosette leaves. RT-PCR proved that in these transgenic seedlings with aberrant rosette leaves [64(38 + 26)/82], endogenous *ASL15/LBD17* expression was completely inhibited (Fig. 1c). These above findings reveal that we have gained successfully transgenic seedlings with antisense *ASL15/LBD17*. These seedlings with abnormal phenotypes were further studied.

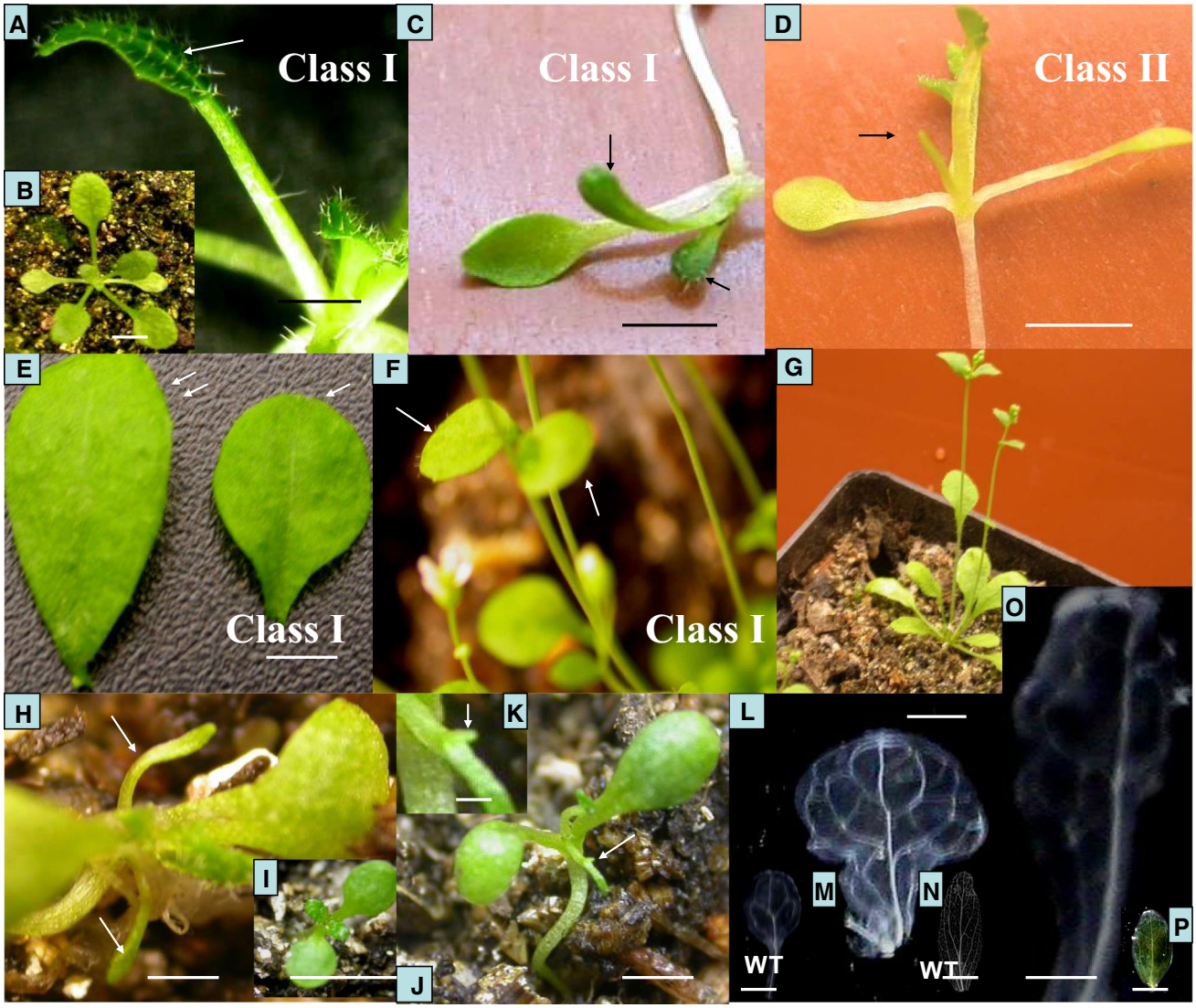

Fig. 2 Phenotypes of transgenic plants with antisense *35S: ASL15*. **a** Sixteen-day-old transgenic plant with antisense *35S:ASL15* showed slightly narrow leaf (class I) (*arrow*). **b** Twenty-five-day-old wild type of *Arabidopsis thaliana* ecotype Columbia. **c** Sixteen-day-old transgenic plant with antisense *35S:ASL15* presents extremely narrow rosette leaves (class I) (*arrow*). **d** Twenty-day-old transgenic plant with antisense *35S:ASL15* presented the radial needle-like rosette leaves (class II) (*arrow*). **e** Thirty-two-day-old cauline leaves of antisense *35S:ASL15* (*arrow*) and wild type (*double arrow*). **f** Thirty-two-day-old antisense *35S:ASL15* transgenic plant with extremely round cauline leaves (*arrow*). **g** Thirty-day-old wild-type *Arabidopsis* (Col-0). **h** In *as2* mutant background, fifteen-day-old transgenic plant with antisense *35S:ASL15* presented extremely narrow rosette leaf (*arrow*). **i** Fifteen-day-old *as2* mutant plant. **j** Fifteen-day-old transgenic plant with antisense *35S:ASL15* presented needle-like leaf (*arrow*). **k** *Arrow* in (**j**) indicates the magnified views of ectopic outgrowth in the adaxial side of needle-like leaf. **l** Vascular pattern of 33-day-old antisense *35S:ASL15/LBD17* cauline leaf. **m** Vascular pattern of 15-day-old wild-type cotyledon. **n** Vascular pattern of 40-day-old wild-type cauline leaf. **o** Vascular pattern of 20-day-old antisense *35S:ASL15/LBD17* narrow rosette leaf. **p** Vascular pattern of 20-day-old wild-type rosette leaf. *Bars* 2.0 mm

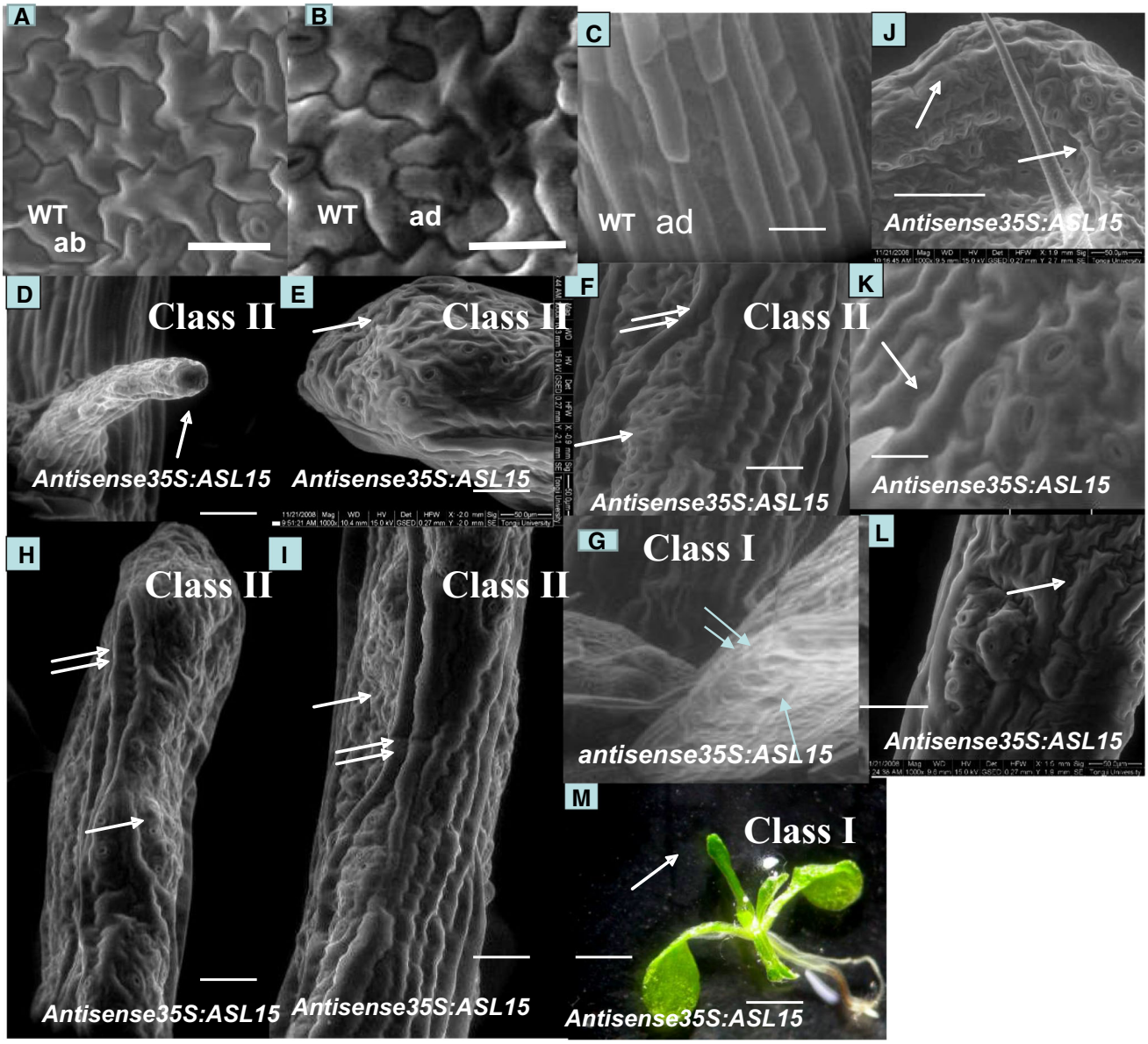

Fig. 3 Antisense *35S: ASL15* shows ab/adaxial polarity defects. **a** Cross section via inflorescence stems of wild type. **b** The magnified views of the regions *boxed* in (**a**). **c** Cross section through the inflorescence stems of wild type. **d** The magnified views of the regions *boxed* in (**c**). **e** Cross section through the slightly narrow rosette leaf of transgenic plant with antisense *35S:ASL15/LBD17*. The magnified views of the regions *boxed* in (**e**). *Bars* 50 um in (**a**), (**c**), and (**e**); 20 um in (**b**), (**d**), and (**f**). *ad* adaxial, *ab* abaxial, *s* spongy mesophyll, *p* palisade mesophyll, *x* xylem, *ph* phloem

Phenotypic alteration of transgenic plants

For better analyze the *ASL15/LBD17* function in the growth and development in *Arabidopsis*, we observed the phenotypes of transgenic seedlings with antisense *35S:ASL15/LBD17*. The rosette leaf blades presented slightly and extremely narrow (class I) and filamentous symmetric and radial needle-like patterning (class II) (Figs. 2a and d arrow; 3m arrow; 4n double arrow), In contrast to those of wild type (Col-0), these abnormal phenotypes of trichomes and stomata (class I) in the transgenic seedlings with antisense *35S:ASL15* imply that *ASL15* might be multiple functions. The reduction of the trichome branching was observed on the narrow rosette leaf blades with antisense *35S:ASL15/LBD17* (class I), to one or two (Fig. 4b, c, d), but not the three to four branches of wild type (Fig. 4a). This trichome also support that cells on leaf blades with antisense *35S:ASL15/LBD17* (class I) are declined in both size and number, and protruded from the leaf blade surface (Fig. 4b, c, d arrowheads), in contrast to those of Col-0 (Fig. 4a arrowheads). For testing the influences of antisense *35S:ASL15* changed the pattern on

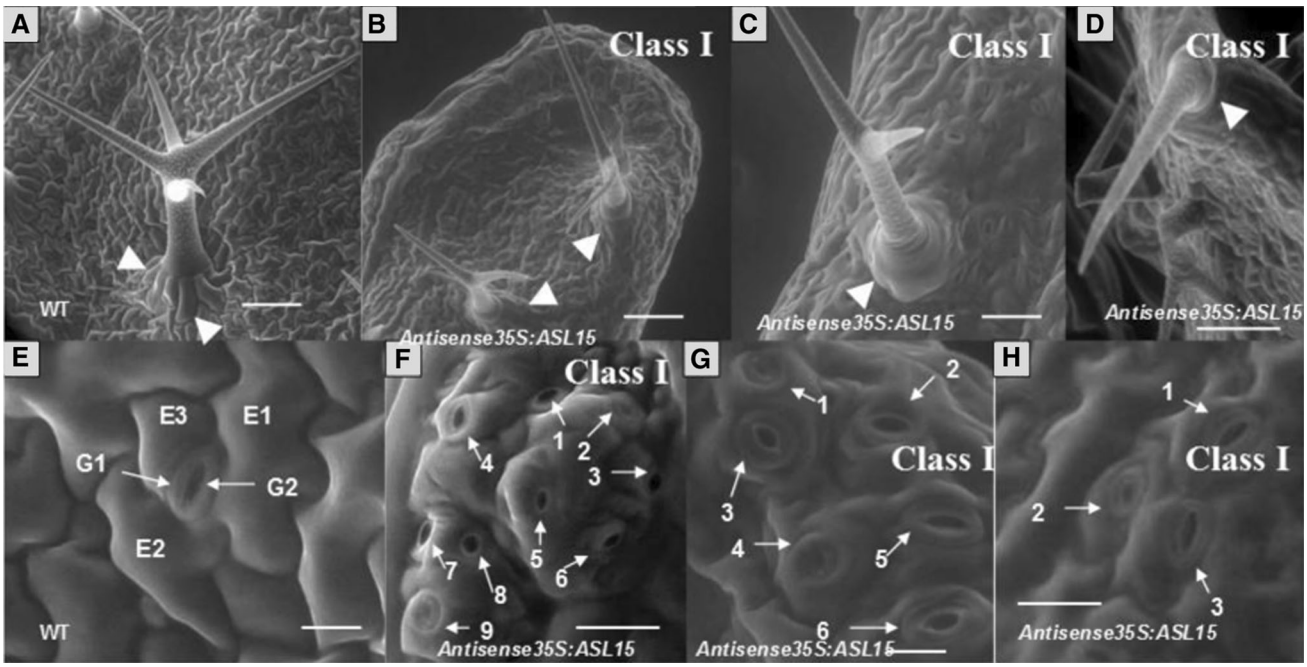

Fig. 4 Antisense *35S:ASL15* leads to both abaxial and adaxial defects of polarity. **a** Cross section through the first rosette leaf or second rosette leaf in a wild type. **b** The magnified views of the regions *boxed* in (**a**), (**c**), (**d**) the base, tip of cross section through the needle-like rosette leaf of transgenic plant with antisense *35S:ASL15/LBD17*, respectively. *Arrow* indicates palisade-like-mesophyll and elongated palisade cells. **e** The needle-like rosette leaf of antisense *35S:ASL15/LBD17*. *Fine thread* indicates the tip of needle-like rosette leaf, and *thick thread* indicates the base of needle-like rosette leaf with the approximate section regions. **f** The magnified views of the *big box* regions in (**c**). **g** Cross section via the dramatically narrow rosette leaf of transgenic plants with antisense *35S:ASL15/LBD17*. *Arrow* indicates that spongy mesophyll cells of irregular shape with ramus, loosely packed, at the both abaxial and adaxial sides. **h** The magnified views of the *small box* regions in (**g**). **i** Cross section via filamentous symmetric leaf with *35S:ASL15/LBD17*. **j** The magnified views of the *small box* regions in **i**. *Bars* 50 um in (**a**), (**c**), (**d**), (**g**), and (**i**); 20 um in (**b**), (**f**), (**h**), and (**j**); 2.0 mm in (**e**). *ad* adaxial, *ab* abaxial, *s* spongy mesophyll, *p* palisade mesophyll, *x* xylem, *ph* phloem

the stomatal development; we analyzed the cell lineage of at least 50 extremely narrow rosette leaf blades (class I). There were 5–8 % stomatal complexes of each line, and these stomatal complexes formed quaternary to sextuple pattern in narrow leaf blades, which were never observed in Col-0 seedlings (data not shown). The stomatal distributions of these narrow rosette leaves (class I) differed significantly from those of wild type (Fig. 4e) and consistently exhibited a dramatic shift to higher order stomatal complexes, in which tertiary on adaxially distal surface (Fig. 4h) and sextuple on adaxially middle surface (Fig. 4g) form predominate. Extremely, adaxially proximal surface showed nonuple stomatal complexes (Fig. 4f). The pleiotropic phenotypes of the seedlings with antisense *35S:ASL15* imply that *ASL15* has multiple functions in the plant development.

Antisense *35S:ASL15/LBD17* presents leaf blade dramatically restricted expanded, implying that it may be a relatively simple model for the determination of abaxial–adaxial axis (Waites and Hudson 1995). Obviously, the filamentous symmetric and needle-like leaf blades (class II) of antisense *35S:ASL15/LBD17* cannot complete further to form laminae. Similar with this, *35S:AS2* transgenic seedlings and the *Arabidopsis phabulosa-1d* (*phb-1d*) mutation exhibited radial needle-like leaf blades, which were thought as being an adaxial cell fate (Lin et al. 2003; McConnell and Barton 1998). Needle-like leaves could not further produce for forming laminae, regardless of the ab/adaxial nature (Xu et al. 2003). Mutations of ab/adaxial polarity typically exhibited the expansion of leaf blades (Bowman et al. 2002), which agree with the model that juxtaposition of ab/adaxial domains is required for leaf blade outgrowth (Waites and Hudson 1995). Thus, during the asymmetric development, enhanced losses are accompanied via declined leaf blade expansion (Eshed et al. 2004).

ASL15/LBD17 determines either adaxial or abaxial cell fate in differently shaped rosette leaves

Cauline leaf blades of antisense *35S:ASL15/LBD17* presented extremely round patterns with simplified vasculature (Fig. 2e arrow, f arrow, l), in contrast to those of Col-0 (Fig. 2e double arrow, g, n). In fact, this vasculature is similar to that of wild-type cotyledon (Fig. 2m). It is well known that cotyledon of *Arabidopsis* is round in shape.

Thus, we speculate whether the leaf shape is determined via vein pattern, that is, it is probable that vein patterning affects the leaf shape. Moreover, in wild-type rosette leaves, the vasculature displayed a reticulate pattern (Fig. 2p), whereas in the antisense *35S:ASL15* narrow rosette leaf blades (class I), midvein often remained and secondary vein drastically simplified (Fig. 2o). While the midvein was still present in these leaf blades, the secondary vein considerably simplified like that in *35S:ASL15* seedlings and implying it is probable that the formation of a vascular network requires the existence of distinct ab/adaxial domains (Lin et al. 2003). Therefore, these alternations of the vasculature may be due to the loss-of-polar expression.

A few evidences have implied that there is a very close link between the antisense *35S:ASL15/LBD17* and the fate of ab/adaxial cells. To address the nature of ab/adaxial features, we characterized the anatomical and morphological polarities of aberrant rosette leaves with *35S:ASL15/LBD17*. In Col-0 leaf blades, tightly packed, elongated palisade mesophyll cells locate at the adaxial side, while spongy mesophyll cells of round or irregular shape with ramus, loosely packed, at the abaxial side (Fig. 5a). These cells of irregular shape with ramus were due to reciprocal drags of abaxial epidermis cells (Avery 1933; Maksymowych 1963). Transverse sections of these radial needle-like leaves (class II) showed uniform radial anatomy, with abaxial sub-epidermal cells resembling the adaxial pattern which exhibits tightly packed, elongated palisade-like-mesophyll cells (Fig. 5c, d, arrow). Similar sub-epidermal cells were observed on the abaxial side of *35S:AS2/LBD6* rosette leaves and *jba-1D* radialized leaves (Lin et al. 2003; Williams et al. 2005). In addition, the abaxial epidermis/adaxial epidermis of these needle-like leaves (class II) was also disturbed in seedlings with *35S:ASL15/LBD17*, always presenting a mixture of ab/adaxial pattern (Fig. 5c, d). Interestingly, transverse sections via the base of these radial needle-like leaves (Fig. 5e, thick thread) revealed a large lacuna on the abaxial side, and on this side, only layer mesophyll cells were developed (Fig. 5c). With transverse sections through the tip of these radial needle-like leaves (Fig. 5e, fine thread), the lacuna was very obviously shrunk, and the abaxial mesophyll cell still showed a layer, whereas the adaxial mesophyll cell layers obviously increased (Fig. 5d). These radial needle-like leaves may be due to the inactive peripheral meristem zone (Tepfer and Chessin 1959). Since the stop of cell differentiation and division proceeds with the proximodistal plane, which is from leaf tip to base (Byrne 2005); in not well-developed leaves, the lacuna of the tip should be larger than that of the base. However, the case is contrary. Thus, the result suggests that antisense *35S:ASL15/LBD17* is defective in proximodistal patterning. These *35S:ASL15/LBD17* filamentous symmetric leaves (class II) showed uniform radial anatomy, with symmetric sub-epidermal cells resembling the adaxial pattern which exhibits tightly packed, elongated palisade-like-mesophyll cell (Fig. 5i). Surprisingly, extremely narrow rosette leaves of antisense *35S:ASL15/LBD17* (class I) presented that spongy mesophyll cells of irregular shape with ramus, loosely packed, at the ab/adaxial side, implying that these leaves might be abaxialized (Fig. 5g). In addition, sub-epidermal cells of slightly narrow rosette leaves (class I) were not visibly different from that of Col-0 leaf (Fig. 6e).

Abaxial polarity/adaxial polarity was obvious via the arrangement of different tissues in the primary vascular bundles of *Arabidopsis* Col-0 leaves. Xylem positioned adaxially, and phloem located abaxially (Fig. 5b). In a transverse section of antisense *35S:ASL15/LBD17* radial needle-like leaves (class II), their primary bundles presented variable xylem/phloem arrangements, that is, phloems situated amid xylems (Fig. 5e, f; Table 1). Interestingly, the lateral bundles of these leaves vanished. Similarly, these *35S:ASL15/LBD17* filamentous symmetric leaves (class II) presented that phloem was surrounded via xylem, in contrast with the collateral arrangement in the vascular bundles of Col-0 leaves (Fig. 5j; Table 1), implying that the filamentous symmetric leaf is adaxialized patterning. To be sure if extremely narrow rosette leaf blades (class I) do show abaxial cell fate, we characterized their anatomical and morphological features of the vascular bundles. As speculated, the patterning of these extremely narrow leaf blades is xylem at the center and phloem on both poles, in contrast with the collateral arrangement of the vascular bundles in Col-0 leaves (Fig. 5h; Table 1). While sub-epidermal cells of slightly narrow rosette leaves (class I) were not visibly different from those of wild-type leaf, the arrangement of their vascular bundles was similar to that of extremely narrow leaf (class I), which was xylem at the center and phloem on both poles (Fig. 6f; Table 1).

Like the internal tissues, polarity defects were also apparent in the epidermal cells of antisense *35S:ASL15/LBD17* plants. By the scanning electron microscopy analysis, the Col-0 abaxial epidermis of blades was characterized via an undulating surface which composed of no uniform sized cell (Fig. 3a), whereas the Col-0 adaxial epidermis of blades was identified via a flat surface which composed of large and uniformly sized cells (Fig. 3b). Adaxial epidermis cells of wild-type petiole were long and rectangular with straight anticlinal walls (Fig. 3c). However, the epidermis of a *35S:ASL15/LBD17* filamentous symmetric leaf (class II) was disturbed, always presenting a mixture of adaxial blade and petiole traits (Fig. 3d, e, f, g, n); in contrast with the collateral arrangement of epidermis in Col-0 leaves. Similarly, the distal, middle, and proximal adaxial epidermis of the needle-like leaves (class II) also

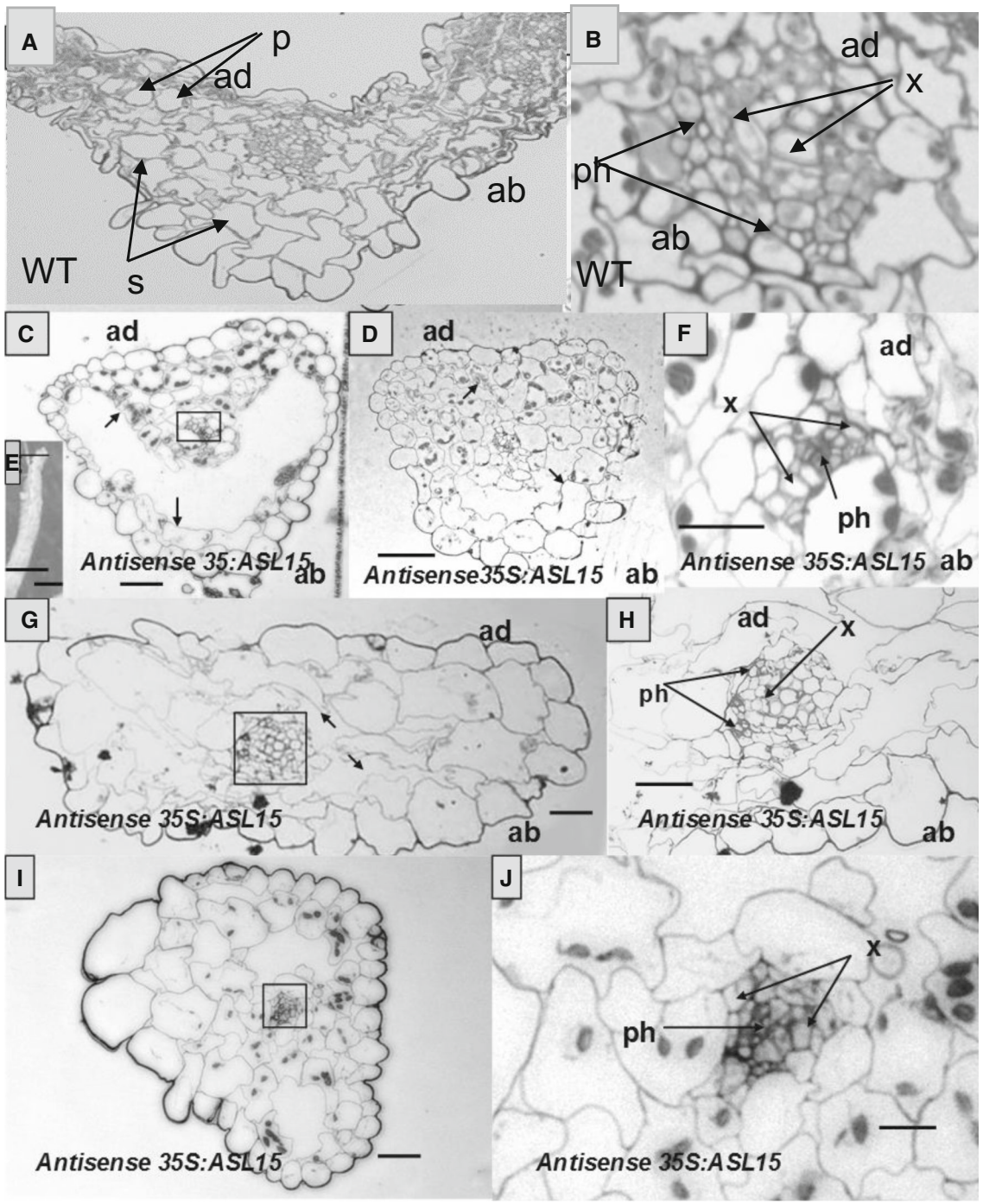

Fig. 5 Epidermal surface of transgenic plants with antisense *35S:ASL15*. **a** Abaxial epidermis of Col-0 rosette leaf exhibiting an undulating surface composed of irregular cell size. **b** Adaxial epidermal cells of a wild-type rosette leaf presenting surface of uniform cell size. **c** Adaxial epidermis cells of Col-0 petiole are rectangular and long with straight anticlinal walls (**d**) filamentous symmetric leaf with *35S:ASL15/LBD17* (*arrow*). **e**, **f**, **g** The tip, middle, and proximal epidermises of *35S:ASL15/LBD17* filamentous symmetric leaf, respectively. *Arrow* indicates the surface of uniform cell size, and *double arrow* indicates the surface with long and rectangular cell. **h, i** The tip or middle and proximal epidermises of *35S:ASL15/LBD17* needle-like leaf, respectively. *Arrow* indicates the surface of uniform cell size, and *double arrow* indicates the surface with long and rectangular cell. **j**, **k**, **l** The tip, middle, and proximal epidermises of adaxial epidermal cells of narrow rosette leaf blades with 35S:ASL15*/LBD17*, respectively. *Arrow* indicates an undulating surface composed of irregular cell size. **m** The transgenic plant with antisense *35S:ASL15/LBD17* presented narrow rosette leaf (*arrow*). **n** The transgenic plant with Antisense *35S:ASL15/LBD17* presented needle-like rosette leaf (*arrow*) and filamentous symmetric leaf (*double arrow*). *Bars* 50 um in (**a**) to (**l**); *Bars* 0.5 cm in (**m**) and (**n**)

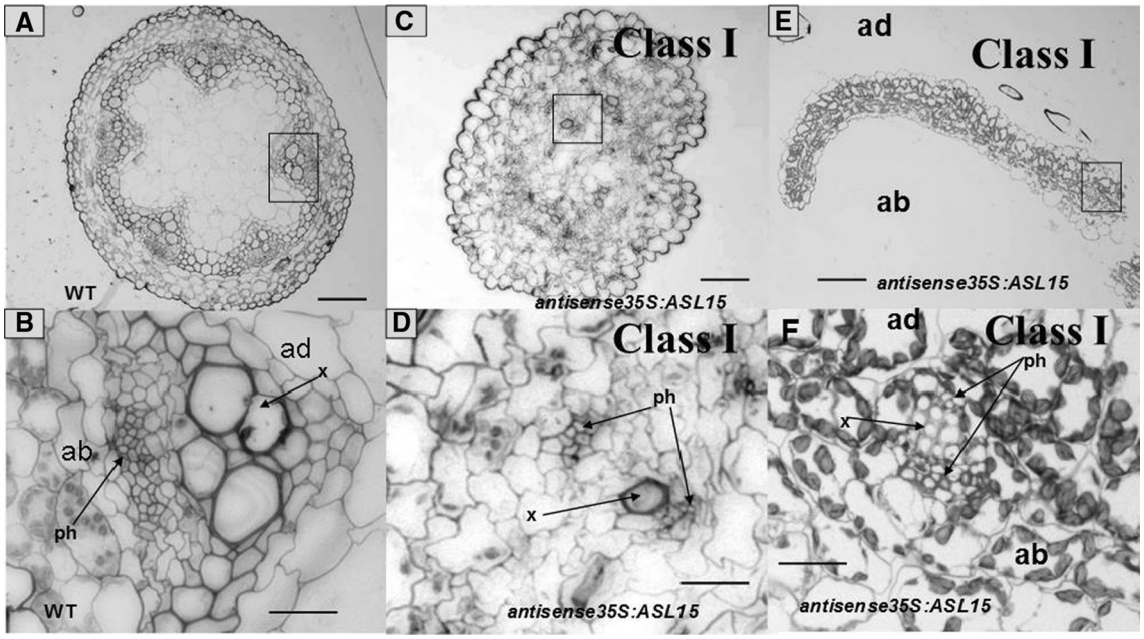

Fig. 6 Epidermal surface of antisense *35S:ASL15* transgenic plants. **a** Wild-type adaxial surface trichomes with four branches. **b**, **c**, **d** are distal adaxial, middle adaxial, and proximal abaxial surfaces on the narrow rosette leaf blades with *35S:ASL15/LBD17* presented trichomes of two, two, and one branches, respectively. *Arrowhead* indicates the trichome support cells. **e** A primary wild-type stomatal complex consisting of a central pair of guard cells (G1 and G2) and stoma surround by neighboring cells (E1, E2, and E3). **f** on the stomatal complexes in the adaxial epidermal cells of the rosette leaf blades with *35S:ASL15/LBD17*, they are nonuple, sextuple, and tertiary, respectively. *Bars* 50 um in (**a**), (**b**), (**c**), and (**d**); *bars* 20 um in (**e**) and (**f**). *Arrows* indicate a primary stomatal complex

Table 1 Percentage of vasculature phenotypes in rosette leaf and inflorescence stem organs

Lines	Total[a]	Normal	Abaxial organ (%)	Partially abaxial organ (%)	Adaxial organ (%)
Rosette leaves					
Col	15	100	0	0	0
Class I[b]	18	33.3	66.7	0	0
Class II[c]	22	27.3	0	0	72.7
as2 Class I[b]	10	0	90	10	0
as2 Class II[c]	10	70	0	30	0
Stems					
Col	10	100	0	0	0
Class I[b]	14	21.4	78.6	0	0
Class II[c]	16	100	0	0	0

[a] Number of organs examined

[b] *35S:ASL15* transgenic plants with narrow leaves

[c] *35S:ASL15* transgenic plants with needle-like or filamentous symmetric rosette leaves

revealed a mixture of adaxial blade and petiole traits (Fig. 3h, i, n). However, the distal, middle, and proximal adaxial epidermis pattern of extremely narrow leaf blades (class I) revealed that an undulating look composed of no uniformly sized cells which are similar to those of wild-type abaxial surface (Fig. 3j, k, l, m), whereas their abaxial surface was not visibly different from that of Col-0 leaves (data not shown). For further identifying the role of *LBD17* in plant development, we obtained a T-DNA insertion mutant from the Salk collection. RT-PCR analysis confirmed that *lbd17* was a knockout allele of *LBD17* (data not shown). *lbd17-1* plants displayed to be very similar to wild-type plants at both seedling and adult stages. Only in the arrangement of the primary vascular bundles, partially abaxialized rosette leaves appeared in *lbd17-1* plants (data not shown); that is, petioles formed half-moon-shaped vasculature, with xylem developing on the inside and phloem on the outside. This was interpreted as partially abaxialized vasculature (Ha et al. 2007). The mild phenotype observed in *lbd17-1* mutant may be attributable to the

functional redundancy of *LBD/ASL* gene family members. These findings imply a redundant role for *ASL15* in promoting abaxial and/or suppressing adaxial cell fate. Similar to *LBD17*, *LBD16* also revealed the same phenomenon (Okushima et al. 2007).

Change of the polarity, positioning, and number of vascular bundles in antisense *35S:ASL15* inflorescence stem

To be sure whether other organ is related to polarity defect, the fasciation phenotype was further examined in the antisense *35S:ASL15* inflorescence stem. In *Arabidopsis* Col-0, the vascular tissue of the stem was present as a ring of five separate bundles (Fig. 6a). The vascular bundles were collateral, with xylem located close to the center of the stem and phloem in more peripheral positions (Fig. 6b). Transverse sections through the antisense *35S:ASL15* Class I inflorescence stem exhibited two types of changes in the vascular patterning. First, antisense *35S:ASL15* stems had more numbers of vascular bundles in peripheral positions along the stem. In addition, the arrangement of peripheral cells was disturbed, in contrast to that of wild type (Col-0) (Fig. 6c). These observations suggest that *ASL15* is important for vascular development. Second, antisense *35S:ASL15* stems showed the defects in the organization of the vascular cell types within these bundles. The wild-type collateral pattern of xylem toward the inside and phloem toward the outside (Fig. 6b) was disrupted in antisense *35S:ASL15* stems by the look of ectopic phloem elements close to the inside (Fig. 6d; Table 1); that is, antisense *35S:ASL15* exhibited xylem at the center and phloem on both poles. Thus, the inflorescence stems of antisense *35S:ASL15* were closely related to abaxial organ identity, which was similar to that of antisense *35S:ASL15* narrow rosette leaf (class I). Though vascular patterning of the antisense *35S:ASL15* Class II inflorescence stem was not visibly different from that of wild-type leaf (Table 1), the arrangement of peripheral cells was disturbed, which was similar to that of the antisense *35S:ASL15* Class I inflorescence stem (data not shown).

Altered expression of the leaf polarity genes in antisense *35S:ASL15* leaves

Phenotypic analyses of antisense *35S:ASL15* indicate that the *ASL15* is required for specifying either abaxial or adaxial identity in differently organ. To better understand if antisense *35S:ASL15* is closely related to either adaxial or abaxial lateral organs of shoots, we attained the molecular evidence of *ASL15* function by examining the mRNA expression of *FIL, YAB3,* and *PHB* genes. It is well known that *FIL* and *YAB3* are responsible for the specialization of abaxial cell fate (Eshed et al. 1999, 2004; Sawa et al. 1999) and *PHB* specifies adaxial cell fate in the lateral organs of *Arabidopsis* (McConnell and Barton 1998). RT-PCR data showed that the expression of these polarity genes is consistent with aberrant phenotype, though their alteration remained unclear if this regulation was direct or indirect. The transcript levels of *YAB3* and *FIL* genes were dramatically increased, and those of *PHB* were dramatically decreased in the *35S:ASL15/LBD17* transgenic plants with narrow rosette leaves (class I), compared with those in wild-type plants (Fig. 7a), whereas the transcript levels of *FIL* gene were invariable, of *YAB3* were slightly decreased, and of *PHB* were dramatically increased in the *35S:ASL15/LBD17* transgenic plants with radial needle-like leaves (class II), compared with those in wild-type plants (Fig. 7a).

While RT-PCR exhibited that the transcript levels of the organ polarity genes were consistent with the aberrant phenotype of *35S:ASL15*, it remained unclear whether the spatial expression patterns of these genes were disturbed. Thus, we examined the expression patterns of the *FIL* polarity gene using RNA in situ hybridization. In wild-type plants, *FIL* expression was restricted to the abaxial side of the developing leaf and apex meristem (Fig. 8a, arrow) (Ha et al. 2007). In *35S:ASL15* transgenic plants with narrow leaves (class I), *FIL* was expressed throughout the entire developing leaf and the apex meristem (Fig. 8d, arrow). However, in *35S:ASL15* transgenic plants with needle-like

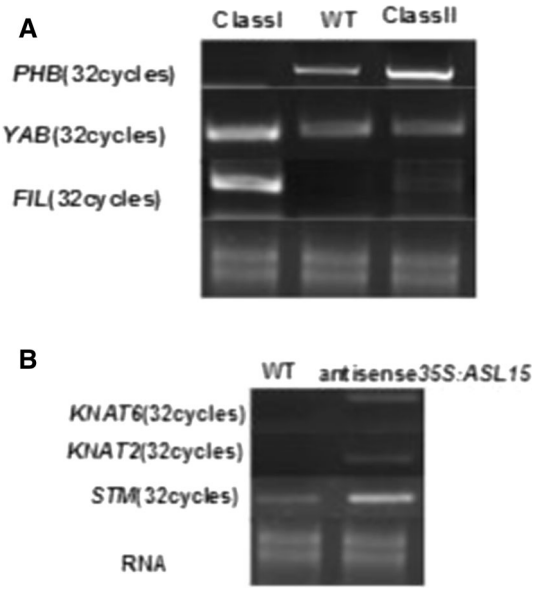

Fig. 7 Some gene expression in transgenic plants with antisense *35S:ASL15*. **a** In transgenic plants with antisense *35S:ASL15*, the gene expressions of *PHB, FIL,* and *YAB3* are altered, in contrast to that of wild type (Col-0). **b** In transgenic plants with antisense *35S:ASL15*, the gene expressions of *KNAT2*, *KNAT6,* and *STM* are increased (**c**), in contrast to those of wild type (Col-0). RNA was used as a control

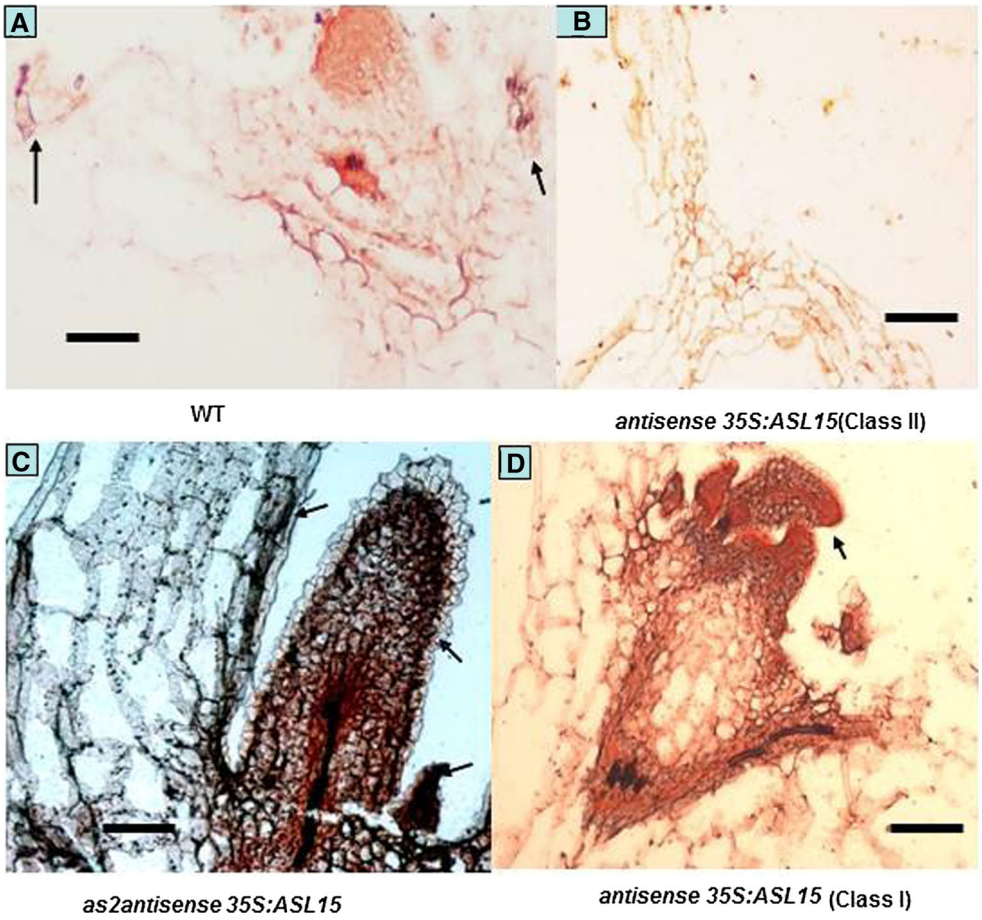

Fig. 8 RNA In Situ Hybridization Analysis of *FIL* Expression. RNA in situ hybridization analysis of *FIL* expression in 10-d-old Col (**a**), antisense *35S:ASL15* class II seedlings (**b**), *as2* antisense *35S:ASL15* antisense seedlings (**c**), and *35S:ASL15* class I seedlings (**d**). *Arrows* indicate the ectopic expression of *FIL*. *Bars* 100 mm

leaves (class II), *FIL* was not expressed in the ab–adaxial side of the developing leaf and the apex meristem (Fig. 8b). These data further support that *ASL15* specifies either abaxial or adaxial cell fate. In general, our data lead to the conclusion that *ASL15/LBD17* is responsible for the specialization of either abaxial or adaxial cell fate in the lateral organs of *Arabidopsis*.

ASL15 antisense overexpression in the *as2-101* mutant background

Mutations in *AS2* confer no clear polarity defects. However, a *35S:AS2/LBD6* transgene did result in leaf polarity defects; the leaves of plants that express this transgene are adaxialized, suggesting a redundant role for *AS2* in promoting adaxial and/or suppressing abaxial cell fate (Lin et al. 2003). To better understand if the effects of *ASL15* antisense overexpression require a functional *AS2* gene, we introduced the *35S:ASL15* transgene into an *as2-1* mutant (Col-0) background. Of 36 *as2-1* plants containing the *35S:ASL15* transgene, 6 resembled *as2-1* single-mutant plants during the whole development (Fig. 2i), whereas the remaining 30 showed novel phenotypes triggered by the *AS15* transgene. In the 30 transgenic plants, 14 with extremely narrow leaf and 16 with needle-like rosette leaf were found (Fig. 2h, j). Of 5 with needle-like rosette leaf reveal the ectopic outgrowth on the adaxial side surface (Fig. 2j, k), which was never found in *35S:ASL15* transgenic plants of wild-type background. These data indicate that the effects of *ASL15* antisense overexpression requires a functional *AS2* gene, and suggest a functional redundancy between these two related *LBDs*. Interestingly, in a transverse section extremely narrow or radial needle-like leaves of *as2-1* antisense *35S:ASL15/LBD17*, their primary bundles all displayed variable xylem/phloem arrangements, i.e., xylems situated amid phloems; however, xylems-surrounding-phloems never were found (Table 1), suggesting *ASL15* only specifies adaxial cell fate in an *as2-1* mutant (Col-0) background. To confirm if *ASL15* specifies adaxial cell fate, we examined the expression patterns of the *FIL* polarity gene using RNA in situ hybridization in *as2* antisense *35S:ASL15* transgenic plants. In *as2* antisense *35S:ASL15* transgenic plants, *FIL* not only expressed in throughout the entire developing leaf but also extended to the adaxial side of mature leaf, which was not observed in mature leaf of *35S:ASL15* plants (Fig. 8c, d, arrow). These results confirm that the effects of *ASL15* antisense overexpression require a functional *AS2* gene.

35S:ASL15/LBD17 results in the upregulation of *KNOX* gene expression

By the RT-PCR analysis, we detected, more or less, the increase levels of *KNAT2*, *KNAT6*, and *STM* transcripts but not of the related *KNAT1* gene in antisense *35S:ASL15/LBD17* plants, compared with those in the wild type (Fig. 7b). However, with typical *KNOX* upregulation, we did not observe aberrant phenotypes in these transgenic plants.

Recent studies in *Arabidopsis thaliana* reveal that the *LBD* gene family can be divided into two groups in terms of the difference of triggering *KNOX* gene expression in lateral organs. (1) Gain-of-function mutant *jlo-D* (*LBD30*) activates the misexpression of the *KNOX* genes *SHOOT MERISTEMLESS* and *KNAT1* in leaves (Borghi et al. 2007). Sense cosuppression and antisense repression of *ASL38/LBD41* resulted in the repression of the *KNOX* genes *KNAT1, KNAT2,* and *KNAT6* in *35S:LBD41* transgenic seedlings (our unpublished data). (2) The expression of *AS2* at high levels triggers the repression of the *KNOX* homeobox genes *BREVIPEDICELLUS*, *KNAT2* and *KNAT6,* but not the related *SHOOT MERISTEMLESS* gene (Lin et al. 2003). In the asymmetric leaves2 (*as2*) mutant of *Arabidopsis thaliana*, transcripts of the *KNAT1*, *KNAT2*, *KNAT6,* and *STM* genes stack in the leaves of *as2* plants, but not in the wild-type plants (Semiarti et al. 2001). *LBD36,* known as *ASL1* (Iwakawa et al. 2002), encodes an LOB domain protein that is closely connected to *AS2*. The overexpression of *LBD36* leads to phenotypes similar to those of *35S:AS2* plants, a result of the repression of *BP* expression. In addition to *Arabidopsis thaliana,* the *PHANTASTICA* (*PHAN*) gene of *Antirrhinum majus* and the *ROUGH SHEATH2* (*RS2*) gene of *Zea mays*, which encode plant homologues of the myb protein (Waites et al. 1998), have been shown to execute the same repression of class I *KNOX* genes (Schneeberger et al. 1998; Timmermans et al. 1999). In *Nicotiana tabacum*, antisense *NSPHAN* leaves show the ectopic expression of *NTH20*, a class I *KNOX* gene (McHale and Koning 2004). The data of the antagonistic or synchronous relationship between ASL/LBD and homeobox members confirm that the harmony of the two gene families is required for the differentiation of lateral organs.

Discussion

In this work, while T-DNA insertions of the expression of *ASL15/LBD17* cannot show obvious defects in plant development except partially abaxialized rosette leaf; we noticed, obvious, the alternations in the lateral organ of antisense overexpression mutants. That is, antisense *35S:ASL15/LBD17* specifies ab/adaxial cell fate in differently shaped rosette leaves of *Arabidopsis*, as well as is defective in proximodistal patterning in the lateral organs of *Arabidopsis*. In the previous reports, *AS1* mutations conferred no clear polarity defects; neither do *as1 as2* double mutations. However, a *35S:AS2/LBD6* transgene does presented leaf polarity defects; the leaves of plants that express this transgene are adaxialized, implying a redundant role for *AS2* in enhancing adaxial and/or suppressing abaxial cell fate (Lin et al. 2003). The phenomenon has also been observed in *LBD16* and *LBD29* (Okushima et al. 2007). RNA interference interruption or T-DNA insertions of the expressions of *LBD16* and *LBD29* did not present any obvious defects in the plant development, for example, lateral root formation. However, the dominant suppression of *LBD16* function significantly suppressed lateral root formation, implying that functional redundancy among *LBD29*, *LBD16*, and other closely related family members might preclude the genetic analysis via using single mutants (Okushima et al. 2007). As mentioned by Okushima et al. (2007), *LBD/ASL* genes might behave duplicated and specialized during evolution. Therefore, these above findings imply that functional redundancy may be an extensive theme in *LBD/ASL* gene family.

In this study, these antisense *35S:ASL15/LBD17* plants revealed the specialization of either abaxial or adaxial cell fate in differently shaped rosette leaves of *Arabidopsis*, namely, these extremely and slightly narrow rosette leaves (class I) presented abaxialized epidermis, sub-epidermis, and vasculature patterning, exhibiting adaxial-to-abaxial transitions, whereas *35S:ASL15* rosette leaves with radical needle-like and filamentous symmetric patterns (class II) revealed adaxialized epidermis, sub-epidermis, and vasculature patterning, showing abaxial-to-adaxial transitions. The inflorescence stems of antisense *35S:ASL15* were closely related to abaxial organ identity, which were similar to that of antisense *35S:ASL15* narrow rosette leaf (class I). This phenomenon indicates that *ASL15/LBD17* is involved in a dual ab/adaxializing function during the lateral organ development. A dual abaxializing/adaxializing has been reported for the *YAB* gene *GRAMINIFOLIA* (*GRAM*), the *Antirrhinum* ortholog of *FIL* (Golz et al. 2004; Navarro et al. 2004). In developing *Antirrhinum* organs, *GRAM* is abaxially expressed, thus is needed for growth at the leaf margins and abaxial cell traits. In addition, the mutation of *GRAM* causes adaxial mesophyll cells, which is away from the leaf margin for resembling partially abaxial cells of the spongy mesophyll. Moreover, occasionally, *gram* plants present radical needle-like leaf blades, where phloem is surrounded via xylem. On the basis of an attractive explanation which the *YABBY* dual ab/adaxializing function, in dorsoventral polarity, the

YABBY role differs between species. It is also possible that in phenotypes of loss-of-function in different species, divergent redundant levels are reflected via differences (Byrne 2005). However, the explanation is not well fit for the dual abaxializing or adaxializing function of antisense *35S:ASL15,* because we have observed the dual abaxializing or adaxializing phenotype within a single species. Our data indicated that differences of loss-of-function phenotypes can also be triggered by the divergence of redundancy in the same species. Furthermore, in *as2-1* mutant background, the abaxial defects of antisense *35S:ASL15* were greatly enhanced compared with those of parental plants. In addition, the adaxial defects of antisense *35S:ASL15* were never found in *as2-1* background. It is probably that in *as2-1* background, abaxal function of *ASL15* is suppressed by adaxial role for *AS2*. Similarly, in contrast with *gram* mutants, *Arabidopsis fil yab3* mutants only reveal adaxialized the lateral organ development (Siegfried et al. 1999). Differently, some *kan1* and *kan2* rosette leaf petioles develop abaxial vasculature (Ha et al. 2007), whereas *kan1, kan2,* and *kan3* stems exhibit adaxial vasculature (Emery et al. 2003). It is largely unclear how and why divergence of redundancy are caused. While functional redundancy is an extensive theme in genetic pathways of regulating polarity (Bowman et al. 2002), only a few redundant divergences have been reported. With more polarity determinator acquired, the phenomenon of redundant divergence can be also common. In antisense *35S:ASL15/LBD17*, it seems that extremely defective phenotype (such as needle-like rosette leaf) (class II) is caused via the loss of ASL15 abaxial activity, and slightly, defective phenotype (such as narrow rosette leaf) (class I) is caused by the loss of ASL15 adaxial activity.

Another dual function is *KAN* gene. Loss of KAN activity reveals leaf adaxialization, implying that the *KAN* specifies abaxial cell fate (Eshed et al. 2001, 2004; Emery et al. 2003). Very recently, the milkweed *pod1* gene, encoding a KANADI protein, specifies the patterning of in maize leaves (Candela et al. 2008). However, Ha et al. (2007) have reported that both *KAN1* and *KAN2* polarity genes act to promote cell fate of adaxiality. The research team performed the molecular and phenotypic effects of *BOP1* and *BOP2* null alleles and overexpression lines in wild-type and different leaf mutant backgrounds. In detail, some rosette leaf petioles of *kan1* and *kan2* mutant produce abaxial vasculature. Moreover, the role of *KAN1* and *KAN2* is significantly increased in the mutant background of *as1*, *as2*, and *bop1, bop2*. Therefore, they believe that *KAN1* and *KAN2* might function to enhance adaxial organ identity, which is redundant with *AS1*, *AS2*, *BOP1*, and *BOP2,* as well as their well-known function of forming abaxial organ identity. On the basis of the dual ab/adaxializing function of *KAN2* and *KAN1*, it is possible that in distinct leaf domains (blade/petiole in *Arabidopsis* or blade/sheath in maize), normal development involved in the same developmental pathways but a distinct explanation of positional signals (Candela et al. 2008). In nature, this interpretation agrees with that of redundant divergence (Byrne 2005). In our work, besides *35S:ASL15* rosette leaves showing polarity defect, inflorescence stems also reveal an abaxialized defect. The wild-type collateral pattern of xylem toward the inside and phloem toward the outside was disrupted in antisense *35S:ASL15* inflorescence stems via the appearance of ectopic phloem elements close to the inside. In addition, antisense *35S:ASL15* stems have more numbers of vascular bundles in peripheral positions along the stem. In other words, these inflorescence stems present xylem at the center and phloem on both poles. Therefore, these inflorescence stems also present abaxial organ identity, which is similar to that of antisense *35S:ASL15* narrow rosette leaves (class II). This implies a defect in the antisense *35S:ASL15* plants in the production, reception, or interpretation of positional signals that pattern the vasculature. It seems that distinct organ (narrow rosette leaf/inflorescence stem) also involved in the same developmental pathways.

Author contributions L.-S. M and J.-H. J. designed experiments. L.-S.M. and Z-B W performed the experiments. L.-S. M, Z.-B. W., X.-Y. C., Y.-B. W, and H.-J. Z. completed the statistical analysis of data. L.-S. M., Z.-B. W, and J.-H. J. wrote, edited, and revised this manuscript.

Acknowledgments We thank Hai Huang for the *as2-101* seeds (Chinese Academy of Sciences, Shanghai, China). This study was also supported by grants from the National Science Foundation of China (31401443, 31370646, and 31560164).

References

Alvarez J, Guli CL, Yu X-H, Smyth DR (1992) Terminal flower: a gene affecting inflorescence development in *Arabidopsis thaliana*. Plant J 2:103–116

Andersson J, Walters RG, Horton P, Jansson S (2001) Antisense inhibition of the photosynthetic antenna proteins CP29 and CP26: implications for the mechanism of protective energy dissipation. Plant Cell 13:1193–1204

Avery GS Jr (1933) Structure and development of the tobacco leaf. Am J Bot 20:565–592

Bao N, Lye KW, Barton MK (2004) MicroRNA binding sites in *Arabidopsis* class III *HD-ZIP* mRNAs are required for methylation of the template chromosome. Dev Cell 7:653–662

Borghi L, Bureau M, Simon R (2007) Arabidopsis *JAGGED LATERAL ORGANS* is expressed in boundaries and coordinates *KNOX* and *PIN* activity. Plant Cell 19:1795–1808

Bowman JL, Eshed Y, Baum SF (2002) Establishment of polarity in angiosperm lateral organs. Trends Genet 18:134–141

Byrne ME (2005) Networks in leaf development. Curr Opin Plant Biol 8:59–66

Byrne ME, Barley R, Curtis M, Arroyo JM, Dunham M, Hudson A, Martienssen RA (2000) Asymmetric leaves1 mediates leaf patterning and stem cell function in *Arabidopsis*. Nature 408:967–971

Candela H, Johnston R, Gerhold A, Foster T, Hake S (2008) The milkweed *pod1* gene encodes a KANADI protein that is required for abaxial/adaxial patterning in maize leaves. Plant Cell 20:2073–2087

Chalfun-Junior A, Franken J, Mes JJ, Marsch-Martinez N, Pereira A, Angenent GC (2005) *ASYMMETRIC LEAVES2- LIKE1* gene, a member of the *AS2/LOB* family, controls proximaldistal patterning in *Arabidopsis* petals. Plant Mol Biol 57:559–575

Chuck G, Lincoln C, Hake S (1996) *KNAT1* induces lobed leaves with ectopic meristems when overexpressed in *Arabidopsis*. Plant Cell 8:1277–1289

Ecker JR, Davis RW (1986) Lnhibition of gene expression in plant cells by expression of antisense RNA. Proc Natl Acad Sci USA 83:5372–5376

Emery JF, Floyd SK, Alvarez J, Eshed Y, Hawker NP, Izhaki A, Baum SF, Bowman JL (2003) Radial patterning of *Arabidopsis* shoots by class III HD-ZIP and KANADI genes. Curr Biol 13:1768–1774

Eshed Y, Baum SF, Bowman JL (1999) Distinct mechanisms promote polarity establishment in carpels of *Arabidopsis*. Cell 99:199–209

Eshed Y, Baum SF, Perea JV, Bowman JL (2001) Establishment of polarity in lateral organs of plants. Curr Biol 11:1251–1260

Eshed Y, Izhaki A, Baum SF, Floyd SK, Bowman JL (2004) Asymmetric leaf development and blade expansion in Arabidopsis are mediated by *KANADI* and *YABBY* activities. Development. 131:2997–3006

Fan M, Xu C, Xu K, Hu Y (2012) LATERAL ORGAN BOUNDARIES DOMAIN transcription factors direct callus formation in Arabidopsis regeneration. Cell Res 22:1169–1180

Ganeteg U, Strand Å, Gustafsson P, Jansson S (2001) Theroperties of the chlorophyll *a/b*-binding proteins Lhca2 and Lhca3 studied in vivo using antisense inhibition. Plant Physio 127:150–158

Golz JF, Roccaro M, Kuzoff R, Hudson A (2004) *GRAMINIFOLIA* promotes growth and polarity of *Antirrhinum* leaves. Development 131:3661–3670

Ha CM, Jun JH, Nam HG, Fletcher JC (2007) *BLADE-ON-PETIOLE1* and 2 control Arabidopsis lateral organ fate through regulation of LOB domain and adaxial-abaxial polarity genes. Plant Cell 19:1809–1825

Hamilton AJ, Lycett GW, Grierson D (1990) Antisense gene that inhibits synthesis of the hormone ethylene in transgenic plants. Nature 346:284–287

Hareven D, Gutfinger T, Parnis A, Eshed Y, Lifschitz E (1996) The making of a compound leaf: genetic manipulations of leaf architecture in tomato. Cell 84:735–744

Hudson A (2000) Development of symmetry in plants. Annu Rev Plant Physiol Plant Mol Biol 51:349–370

Iwakawa H, Ueno Y, Semiarti E, Onouchi H, Kojima S, Tsukaya H, Hasebe M, Soma T, Ikezaki M, Machida C, Machida Y (2002) The *ASYMMETRIC LEAVES2* gene of *Arabidopsis thaliana*, required for formation of a symmetric flat leaf lamina, encodes a member of a novel family of proteins characterized by cysteine repeats and a leucine zipper. Plant Cell Physiol 43:467–478

Jackson D, Veit B, Hake S (1994) Expression of maize *KNOTTED1* related homeobox genes in the shoot apical meristem predicts patterns of morphogenesis in the vegetative shoot. Development 120:405–413

Kim J, Jung JH, Reyes JL, Kim YS, Kim SY, Chung KS, Kim JA, Lee M, Lee Y, Kim VN, Chua NH, Park CM (2005) MicroRNA cleavage of *ATHB15* mRNA regulates vascular development in *Arabidopsis* inflorescence stems. Plant J 42:84–94

Lin WC, Shuai B, Springer PS (2003) The Arabidopsis *LATERAL ORGAN BOUNDARIES*-domain gene *ASYMMETRIC LEAVES2* functions in the repression of KNOX gene expression and in adaxial-abaxial patterning. Plant Cell 15:2241–2252

Lincoln C, Long J, Yamaguchi J, Serikawa K, Hake S (1994) A *Knotted1*-like homeobox gene in *Arabidopsis* is expressed in the vegetative meristem and dramatically alters leaf morphology when overexpressed in transgenic plants. Plant Cell 6:1859–1876

Liu J, Sheng L, Xu Y, Li J, Yang Z, Huang H, Xu L (2014) *WOX11* and *12* are involved in the first-step cell fate transition during de novo root organogenesis in Arabidopsis. Plant Cell 26:1081–1093

Long JA, Moan EI, Medford JI, Barton MK (1996) A member of the *KNOTTED* class of homeodomain proteins encoded by the *SHOOTMERISTEMLESS* gene of *Arabidopsis*. Science 379:66–69

Maksymowych R (1963) Cell division and cell elongation in leaf development of *Xantium pensylvanicum*. Am J Bot 50:891–901

McConnell JR, Barton MK (1998) Leaf polarity and meristem formation in *Arabidopsis*. Development 125:2935–2942

McConnell JR, Emery J, Eshed Y, Bao N, Bowman J, Barton MK (2001) Role of *PHABULOSA* and *PHAVOLUTA* in determining radial patterning in shoots. Nature 411:709–713

McHale NA, Koning RE (2004) *PHANTASTICA* regulates development of the adaxial mesophyll in *Nicotiana* leaves. Plant Cell 16:1251–1262

Meng LS (2015) Transcription coactivator Arabidopsis ANGUSTIFOLIA3 modulates anthocyanin accumulation and light-induced root elongation through transrepression of constitutive photomorphogenic1. Plant Cell Envir 38:838–851

Meng LS, Yao SQ (2015) Transcription co-activator Arabidopsis ANGUSTIFOLIA3 (AN3) regulates water-use efficiency and drought tolerance by modulating stomatal density and improving root architecture by the transrepression of YODA (YDA). Plant Biotechnol J 13:893–902

Meng LS, Song JP, Sun SB, Wang CY (2009) The ectopic expression of *PttKN1* gene causes pleiotropic alternation of morphology in transgenic carnation (*Dianthus caryophyllus* L.). Acta Physiol Plant 31:1155–1164

Meng LS, Wang YB, Yao SQ, Liu A (2015a) Arabidopsis AINTEGUMENTA (ANT) mediates salt tolerance by transrepressing SCABP8. J Cell Sci 128:2919–2927

Meng LS, Wang ZB, Yao SQ, Liu A (2015b) The ARF2–ANT–COR15A gene cascade regulates ABA signaling-mediated resistance of large seeds to drought in Arabidopsis. J Cell Sci 128:3922–3932

Navarro C, Efremova N, Golz JF, Rubiera R, Kuckenberg M, Castillo R, Tietz O, Saedler H, Schwarz-Sommer Z (2004) Molecular and genetic interactions between *STYLOSA* and *GRAMINIFOLIA* in the control of Antirrhinum vegetative and reproductive development. Development 131:3649–3659

Nishimura A, Tamaoki M, Sato Y, Matsuoka M (1999) The expression of tobacco *knotted1*-type class 1 homeobox genes correspond to regions predicted by the cytohistological zonation model. Plant J. 18:337–347

Oeller PW, Min-Wong L, Taylor LP, Pike DA, Theologis A (1991) Reversible inhibition of tomato fruit senescence by antisense RNA. Science 254:437–439

Okushima Y, Fukaki H, Onoda M, Theologis A, Tasaka M (2007) *ARF7* and *ARF19* regulate lateral root formation via direct activation of *LBD/ASL* genes in *Arabidopsis*. Plant Cell 19:118–130

Prigge MJ, Otsuga D, Alonso JM, Ecker JR, Drews GN, Clark SE (2005) Class III homeodomain-leucine zipper gene family members have overlapping, antagonistic, and distinct roles in *Arabidopsis* development. Plant Cell 17:61–76

Rothstein SJ, DiMaio J, Strand M, Rice D (1987) Stable and heritable inhibition of the expression of nopaline synthase in tobacco expressing antisense RNA. Proc Natl Acad Sci USA 84:8439–8443

Sawa S, Watanabe K, Goto K, Kanaya E, Morita EH, Okada K (1999) *FILAMENTOUS FLOWER*, a meristem and organ identity gene of *Arabidopsis*, encodes a protein with a zinc finger and HMG-related domains. Genes Dev 13:1079–1088

Schneeberger RG, Becraft PW, Hake S, Freeling M (1995) Ectopic expression of the *knox* homeo box gene *rough sheath1* alters cell fate in the maize leaf. Genes Dev 9:2292–2304

Schneeberger R, Tsiantis M, Freeling M, Langdale JA (1998) The *ROUGH SHEATH2* gene negatively regulates homeobox gene expression during maize leaf development. Development 125:2857–2865

Semiarti E, Ueno Y, Tsukaya H, Iwakawa H, Machida C, Machida Y (2001) The *ASYMMETRIC LEAVES2* gene of *Arabidopsis thaliana* regulates formation of a symmetric lamina, establishment of venation and repression of meristem-related homeobox genes in leaves. Development 128:1771–1783

Sentoku N, Sato Y, Kurata N, Ito Y, Kitano H, Matsuoka M (1999) Regional expression of the rice *kn1*-type homeobox gene family during embryo, shoot, and flower development. Plant Cell 11:1651–1664

Sentoku N, Sato Y, Matsuoka M (2000) Overexpression of rice *OSH* genes induces ectopic shoots on leaf sheaths of transgenic rice plants. Dev Biol 220:358–364

Shuai B, Reynaga-Peña CG, Springer PS (2002) The *LATERAL ORGAN BOUNDARIES* gene defines a novel, plant-specific gene family. Plant Physiol 129:747–761

Siegfried KR, Eshed Y, Baum SF, Otsuga D, Drews GN, Bowman JL (1999) Members of the YABBY gene family specify abaxial cell fate in Arabidopsis. Development 126:4117–4128

Sinha NR, Williams RE, Hake S (1993) Overexpression of the maize homeobox gene, *KNOTTED-1*, causes a switch from determinate to indeterminate cell fates. Genes Dev 7:787–795

Smith CJS, Watson CF, Ray J, Blrd CR, Morris PC, Schuch W, Grierson D (1988) Antisense RNA inhibition of polygalacturonase gene expression in transgenic tomatoes. Nature 334:724–726

Tamaoki M, Kusaba S, Kano-Murakami Y, Matsuoka M (1997) Ectopic expression of a tobacco homeobox gene, *NTH15*, dramatically alters leaf morphology and hormone levels in transgenic tobacco. Plant Cell Physiol 38:917–927

Tang G, Reinhart BJ, Bartel DP, Zamore PD (2003) A biochemical framework for RNA silencing in plants. Genes Dev 17:49–63

Tepfer SS, Chessin M (1959) Effects of tobacco mosaic virus on early leaf development in tobacco. Am J Bot 46:496–509

Timmermans MCP, Hudson A, Becraft PW, Nelson T (1999) ROUGH SHEATH2: a Myb protein that represses *knox* homeobox genes in maize lateral organ primordia. Science 284:151–153

Tzfira T, Jensen CS, Wang W, Zuker A, Vinocur B, Altman A, Vainstein A (1997) Transgenic *Populus tremula*: a step-by-step protocol for its *Agrobacterium*-mediated transformation. Plant Mol Biol Rep 15:219–235

Van der Krol AR, Lenting PE, Veenstra J, Van der Meer IM, Koes RE, Gerats AGM, Moi JNM, Stuitje AR (1988) An anti-sense chalcone synthase gene in transgenic plants inhibits flower pigmentation. Nature 333:866–869

Waites R, Hudson A (1995) *Phantastica*: a gene required for dorsiventrality of leaves in *Antirrhinum majus*. Development 121:2143–2154

Waites R, Selvadurai HRN, Oliver IR, Hudson A (1998) The PHANTASTICA gene encodes a MYB transcription factor involved in growth and dorsoventrality of lateral organs in Antirrhinum. Cell 93:779–789

Williams L, Grigg SP, Xie M, Christensen S, Fletcher JC (2005) Regulation of *Arabidopsis* shoot apical meristem and lateral organ formation by microRNA miR166 and its *AtHD-ZIP* target genes. Development 132:3657–3668

Xu L, Xu Y, Dong A, Sun Y, Pi L, Xu Y, Huang H (2003) Novel *as1* and *as2* defects in leaf adaxial-abaxial polarity reveal the requirement for *ASYMMETRIC LEAVES1* and 2 and *ERECTA* functions in specifying adaxial identity. Development 130:4097–4107

Zhang H, Goodman HM, Jansson S (1997) Antisense inhibition of the photosystem I antenna protein Lhca4 in *Arabidopsis thaliana*. Plant Physiol 115:1525–1531

Zhong RQ, Ye ZH (2004) Amphivasal vascular bundle 1, a gain -of-function mutation of the *IFL1/REV* gene, is associated with alterations in the polarity of leaves, stems and carpels. Plant Cell Physiol 45:369–385